

Estimating rainfall erosivity by incorporating seasonal variations in parameters into the Richardson model

WANG Yousheng^{1,2}, TAN Shi^{1,3}, *LIU Baoyuan¹, YANG Yang¹

1. State Key Laboratory of Earth Surface Processes and Resources Ecology, Beijing Normal University, Beijing 100875, China;

2. State Key Laboratory of Simulation and Regulation of Water Cycle in River Basin, China Institute of Water Resources and Hydropower Research, Beijing 100048, China;

3. College of Education Science, Hunan First Normal University, Changsha 410205, China

Abstract: Rainfall erosivity is an important climatic factor for predicting soil loss. Through the application of high-resolution pluviograph data at 5 stations in Huangshan City, Anhui Province, China, we analyzed the performance of a modified Richardson model that incorporated the seasonal variations in parameters α and β . The results showed that (1) moderate to high seasonality was presented in the distribution of erosive rainfall, and the seasonality of rainfall erosivity was even stronger; (2) seasonal variations were demonstrated in both parameters α and β of the Richardson model; and (3) incorporating and coordinating the seasonality of parameters α and β greatly improved the predictions at the monthly scale. This newly modified model is therefore highly recommended when monthly rainfall erosivity is required, such as, in planning soil and water conservation practices and calculating the cover-management factor in the Universal Soil Loss Equation (USLE) and Revised Universal Soil Loss Equation (RUSLE).

Keywords: seasonal rainfall erosivity; Richardson model; cover-management factor; USLE; RUSLE

1 Introduction

Soil loss is one of the most widespread forms of soil degradation (Pimentel *et al.*, 1995; Lal, 2003). The Universal Soil Loss Equation (USLE) and the Revised Universal Soil Loss Equation (RUSLE) are empirical models that have been devised for soil loss predictions (Wischmeier and Smith, 1978; Renard *et al.*, 1997), and these models have been widely used because of their simplicity, even though they are not physically based (Kinnell, 2010). As a

Received: 2015-12-07 **Accepted:** 2016-03-04

Foundation: Fund for Creative Research Groups of National Natural Science Foundation of China, No.41321001; the National Natural Science Foundation of China, No.51379008; the Open Research Fund of the State Key Lab of Simulation and Regulation of Water Cycle in River Basin, No.2014QN04

Author: Wang Yousheng (1987–), PhD Candidate, specialized in soil erosion modeling. E-mail: yswang@mail.bnu.edu.cn

***Corresponding author:** Liu Baoyuan (1958–), Professor, specialized in soil erosion mechanism, soil erosion modeling and regional soil erosion survey technology. E-mail: baoyuan@bnu.edu.cn

numerical description of climate impacts on soil loss, rainfall erosivity is one of the most important factors in the USLE and RUSLE, i.e., it quantifies the potential of rainfall to cause soil loss (Wischmeier and Smith, 1958; Hoyos *et al.*, 2005). Seasonal rainfall erosivity, which is a component of rainfall erosivity, is a factor of importance in calculations of the cover-management factor (C-factor) in the USLE and the RUSLE (Eq. 1) (Wischmeier and Smith, 1978; Guo *et al.*, 2015); it is also widely used in urban and forestry applications for determining soil erosion hazards, predicting the effectiveness of erosion-control activities, and evaluating the impacts of soil erosion potentials under climate change (Yu and Rosewell, 1996; Yu, 1998). The relevant equation is as follows:

$$C = \sum_{i=1}^n SLR_i R_i / R, \quad (1)$$

where C is the cover and management factor, SLR_i is the soil-loss ratio for the time period i , R_i is the rainfall erosivity occurring during that time period (MJ mm/ha/h), n is the number of periods used in the summation, and R is the long-term mean annual rainfall erosivity (MJ mm/ha/h/a).

Generally, long-term pluviograph data are needed to calculate rainfall erosivity (Wischmeier and Smith, 1978; Renard *et al.*, 1997), but often these data are not available for many sites around the world. Consequently, substitutable data can be applied to establish linkages with rainfall erosivity. For example, event rainfall (Richardson *et al.*, 1983; Mannaerts and Gabriels, 2000; Shamshad *et al.*, 2008), daily rainfall (Selker *et al.*, 1990; Davison *et al.*, 2005; Salako, 2010; Sanchez-Moreno *et al.*, 2014), monthly rainfall (Renard and Freimund, 1994; Taguas *et al.*, 2013), and annual rainfall (Mikhailova *et al.*, 1997; Mati *et al.*, 2000; Eltaif *et al.*, 2010; Bonilla and Vidal, 2011; Lee and Heo, 2011) have all been used. While these types of data can solve the issue of limited data and rainfall erosivity estimations on an annual scale, rainfall erosivity estimation on a sub-annual (seasonal, monthly) scale is still problematic.

In order to cope with rainfall erosivity estimation on a sub-annual scale, Petkovsek and Mikos (2004) established 12 rainfall erosivity models, one for each month in a year, based on the power function model (Eq. 2) proposed by Richardson *et al.* (1983) shown below:

$$R_m = a \sum_{k=1}^N P_k^\beta \quad (2)$$

Hoyos *et al.* (2005) also established sub-annual rainfall erosivity models—one for the dry season and one for the rainy season. In view of the differences in monthly rainfall characteristics and impacts of topography on rainfall, Diodato and Bellocchi (2007) developed a monthly rainfall erosivity model based on the monthly rainfall, elevation, and latitude. Kavian *et al.* (2011) modeled the rainfall erosivity for each season: winter, spring, summer, and autumn. As a whole, building rainfall erosivity models for each month or season can yield good estimations, but this requires long-term pluviograph data. In addition, model construction may introduce a large amount of additional parameters that require more datasets to be sourced. In consideration of the seasonal changes of rainfall characteristics, such as the rainfall amount and rainfall intensity, Yu and Rosewell (1996) added a cosine function to parameter α based on the model proposed by Richardson *et al.* (1983). This method reduced the 24 parameters produced by the Richardson model for each month to 6 (Eq.3), thus

solving the problem of the overabundance of parameters. The relevant equation is as follows:

$$R_j = \alpha[1 + \eta \cos(2\pi fj - \omega)] \sum_{k=1}^N P_k^\beta \quad (3)$$

The Yu and Rosewell model (Yu and Rosewell, 1996) was then applied and tested in South Australia (Yu and Rosewell, 1996), the Australian tropics (Yu, 1998), two watersheds in the humid tropics of Australia (Yu and Neil, 2000), Peninsular Malaysia (Yu *et al.*, 2001), China (Guo *et al.*, 2001; Ning and Shi, 2003; Zhu and Yu, 2015), and the whole of Australia (Lu and Yu, 2002), as well as New South Wales in Australia (Yang, 2014).

Study results showed that, by adding a cosine function to parameter α , the data could perfectly represent seasonal variations in parameter α , but large errors still existed in some months, especially in the months with less rainfall. Angulo-Martinez and Begueria (2009) further tried to incorporate seasonal representations of parameter β . Their results showed that prediction errors by the model that incorporated the seasonal variations in both parameters α and β exceeded that with only 1 parameter α . This was contrary to expectation because that the model that considered seasonal variations in only 1 parameter was a special case of the model incorporating 2 parameters and simply held the other constant. Theoretically, a model that incorporates seasonal variations in both parameters α and β could represent more details of the rainfall erosivity. Improvement in predictions is possible if seasonal variations in the 2 parameters are both incorporated and coordinated, in the months with both more and less rainfall.

In order to improve the rainfall erosivity estimation on a monthly scale, by using the rainfall data in high-temporal resolution at 5 stations in Huangshan City, the objectives of this paper were to (1) analyze the seasonal characteristics of erosive rainfall and rainfall erosivity and (2) test the performance of the following 3 model types that incorporated the seasonal variations in parameters into the Richardson model: (a) only considering the seasonal variations in parameter α , with parameter β held constant; (b) only considering the seasonal variations in parameter β , with parameter α held constant; (c) incorporating and coordinating the seasonal variations in both parameters α and β . Results of the work have the potential to improve the approximation of the cover-management factor and soil loss estimations in the USLE and RUSLE.

2 Materials and methods

2.1 Study area and data

Huangshan City is located in the subtropical monsoon climate zone (Figure 1), and it has a warm climate and abundant rainfall. The annual temperature is 15.5–16.4°C, and the annual rainfall range is 900–1700 mm, most of which occurs in June and July. Because of the impact of the East Asian atmospheric circulation, the Meiyu period occurs from mid-June to mid-July, and is characterized by high temperatures, high humidity, and continuous rain. Mountains and hills are the predominant landforms in the region, and the soil on the steep slopes is prone to loss. The region is the urban drinking water source for Huangshan City and the northern Zhejiang Province, so soil loss and water quality in the region are matters

of great concern.

In Huangshan City, data on 2089 erosive rainfall events at a total of 5 rainfall stations with a resolution of 1 minute were collected (Table 1). At 4 stations (Rucun, Siqian, Taiping, and Hezhuang), the rainfall series length exceeded 18 years, and the datasets included over 420 rainfall events. Rainfall series length at the fifth station (Wucheng) was 8 years, and the dataset contained over 200 rainfall events. All these data were used for optimization of seasonal α and β , and comparing model estimated rainfall erosivity with EI_{30} (typical rainfall erosivity calculated method). Siphon rain gauges were used to obtain the pluviograph records, which were then digitized to extract the 1-minute rainfall data.

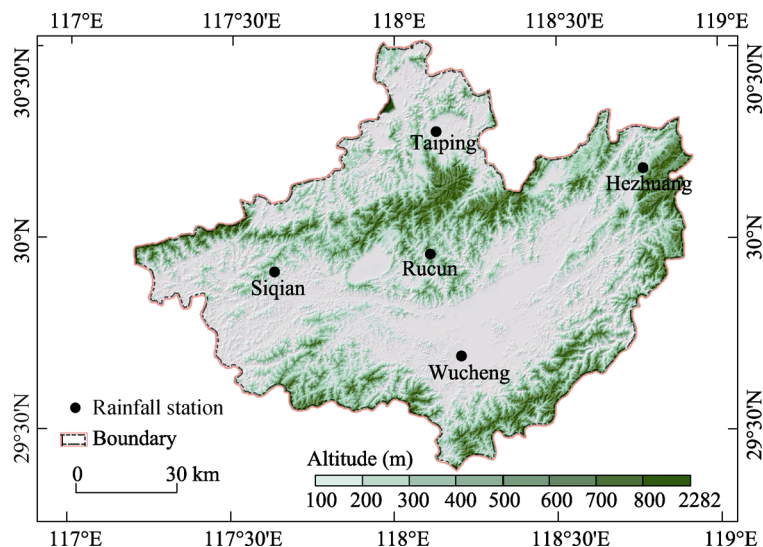


Figure 1 Map showing geographical location of the study area and distribution of rainfall stations

Table 1 Characteristics of rainfall data at the 5 stations in Huangshan City

Station	Period	Years	<i>ERE</i>	Resolution	Altitude	Annual rainfall	Annual <i>R</i>
Rucun	1989–2008	20	522	1	533	1513	7749
Siqian	1989–2008	20	423	1	317	1207	6901
Taiping	1989–1999 2001–2008	19	500	1	200	1326	6090
Hezhuang	1989–2003 2005–2007	18	442	1	450	1369	6507
Wucheng	2000–2005 2007–2008	8	201	1	150	1423	6940
Total		85	2088				

ERE = erosive rainfall events; *R* = rainfall erosivity.

Units: *ERE* (events); resolution (minutes); altitude (m); annual rainfall (mm); annual *R* (MJ mm/ha/h/a)

2.2 Rainfall erosivity calculation

EI_{30} is an abbreviation for energy multiplied by the maximum intensity in 30-minute rainfall events from high-resolution pluviograph records (Eq. 4) (Wischmeier and Smith, 1978). The annual rainfall erosivity (*R*) is the sum of individual storm EI_{30} values for a year, and the

monthly rainfall erosivity (R_m) is the sum of EI_{30} values for a month. The relevant equation is as follows:

$$EI_{30} = \left(\sum_{r=1}^o e_r v_r \right) \cdot I_{30}, \quad (4)$$

where e = unit energy (MJ/mm/ha); v_r = amount of rainfall in the r th period (mm); and I_{30} = maximum 30-minute rainfall intensity (mm/h), which is the average intensity over the continuous 30 minutes with the most rainfall in the storm. e_r is computed as follows (McGregor and Mutchler, 1976; Foster, 2004):

$$e_r = 0.29[1 - 0.72 \exp(-0.082i_r)], \quad (5)$$

where i_r = rainfall intensity for the r th period (mm/h).

The following erosive rainfall criteria (Wischmeier and Smith, 1978) were used to categorize storms: (1) data for storms more than 12.7 mm; (2) rainfall when at least 6.35 mm of rainfall fell in 15 minutes; and (3) a period with less than 1.27 mm in over 6 hours was used to divide a longer storm period into 2 storms.

2.3 Seasonality analysis

In order to quantify the seasonality of erosive rainfall and rainfall erosivity, the concentration index (CI) (Eq. 6) (Oliver, 1980) was employed to analyze the seasonal distributions of the data. The CI classification was as follows (Oliver, 1980): uniform ($8.3 \leq CI < 10.0$), moderately seasonal ($10 \leq CI < 15$), seasonal ($15 \leq CI < 20$), highly seasonal ($20 \leq CI < 50$), and irregular ($50 \leq CI < 100$). A lower CI indicates a more even distribution of rainfall or rainfall erosivity in a year. In contrast, a larger CI suggests that there is centrality or seasonality of rainfall or rainfall erosivity in a year. The CI is calculated as:

$$CI = 100 \sum_{m=1}^{12} \left(\frac{P_m^2}{P_y^2} \right), \quad (6)$$

where P_m = erosive rainfall (or rainfall erosivity) of the m th month and P_y = annual erosive rainfall (or annual rainfall erosivity) of the y th year.

The 4 seasons were classified as winter (December, January, February), spring (March, April, May), summer (June, July, August), and autumn (September, October, November).

2.4 Seasonal rainfall erosivity models

The base model in this study was the Richardson model (Model A) (Eq. 2) (Richardson *et al.*, 1983). A periodic cosine function was added to parameter α , parameter β , and both parameters α and β to obtain the new models B, C, and D, respectively. Model B exhibited seasonal variations in parameter α , with parameter β held constant. Model C had seasonal variations in parameter β , with parameter α held constant, and it was in the form of the Yu and Rosewell model. Model D had seasonal variations in the 2 parameters α and β .

The values of the periodic models added to parameter α and parameter β were not the same, and so F_α (Eq. 7) and F_β (Eq. 8) were introduced to represent the periodicity of parameter α and parameter β , respectively. The relevant equations are as follows:

$$F_\alpha = 1 + \eta_\alpha \cos(2\pi f t + \omega_\alpha) \quad (7)$$

$$F_{\beta} = 1 + \eta_{\beta} \cos(2\pi f_j + \omega_{\beta}) \quad (8)$$

$$\text{Model A:} \quad R_m = \alpha \sum_{k=1}^N P_k^{\beta}, \quad (9)$$

where R_m = rainfall erosivity of the m th month (MJ mm/ha/h); P_k = daily rainfall of the k th erosive rainfall day (mm) (erosive rainfall was set at 12.7 mm); N = erosive rainfall days in the m th month; and α and β are parameters to be computed. The other models are:

$$\text{Model B:} \quad R_m = \alpha \cdot F_{\alpha} \cdot \sum_{k=1}^N P_k^{\beta} \quad (10)$$

$$\text{Model C:} \quad R_m = \alpha \cdot \sum_{k=1}^N P_k^{\beta \cdot F_{\beta}} \quad (11)$$

$$\text{Model D:} \quad R_m = \alpha \cdot F_{\alpha} \sum_{k=1}^N P_k^{\beta \cdot F_{\beta}} \quad (12)$$

The following parameters were used in Model B, Model C, and Model D: α , β , η (η_{α} , η_{β}), ω (ω_{α} , ω_{β}). Parameter α was the rainfall erosivity level of each month; the absolute value of α was of importance to the unbiased estimation of rainfall erosivity. Parameter β illustrated the non-linear relationship between the rainfall amount and rainfall erosivity. Parameter α and parameter β were closely related (Zhu and Yu, 2015). Parameter η represented the influence of rainfall on the seasonality of rainfall erosivity, but it did not influence the overall level of rainfall erosivity. Value ranges of the 3 parameters were $\alpha > 0$, $\beta > 1$, and $0 \leq \eta \leq 1$. Parameter ω represented peak erosivity. In Huangshan City, the Meiyu period occurs from mid-June to mid-July, when there is typically the peak rainfall amount and rainfall erosivity in a year. Meanwhile, the distribution of rainfall erosivity showed a right-skewed trend, and so parameter ω was designated as $5.80\pi/6$ for Model B and Model C after trials, which represented the seasonal distribution of rainfall erosivity well. For Model D, ω_{α} was the same as ω in Model B and Model C, while ω_{β} was computed through parameter fitting.

2.5 Model parameter fitting and precision comparison

Two types of models were used in this study, namely the Richardson model (Model A) and its derivative models (Model B, Model C, and Model D). The least-squares method was applied to estimate parameters of Model A. The Trust-Region-Reflective algorithm was employed in Matlab v.2013b for the derivational models (Model B, Model C, and Model D) to ensure minimal errors (Coleman and Li, 1996; MathWorks, 2005).

Following parameter estimation, it is important to assess the model prediction error because the design of the models will ultimately influence the estimates of rainfall erosivity. A set of goodness-of-fit statistics was used for this purpose (Table 2), and the endpoints were listed as follows. (1) *Mean* = mean value of the observed monthly rainfall erosivity and the model predictions (estimated *mean* of the monthly rainfall erosivity), as well as the annual ones (*mean* of the annual rainfall erosivity). These values represent the closeness between model predictions and observed rainfall erosivity; the relevant unit is MJ mm/ha/h. (2) Mean absolute percentage error (*MAPE*): this was used to assess the mean prediction accuracy of the models. Smaller *MAPE* values are associated with higher model prediction accuracies;

the relevant unit is %. (3) Model efficiency (*ModEff*) (Nash and Sutcliffe, 1970): this is an index that represents the comprehensive performance of the models. It is similar to the coefficient of determination r^2 , but it is less sensitive to outliers; thus, it can compensate for the drawbacks (higher sensitivity to outliers) of the r^2 . The range of the *ModEff* is $-\infty$ to 1. Values of *ModEff* that are closer to 1 are indicative of higher model efficiencies. (4) Mean bias error (*MBE*): this is an index that represents the left or right skew of the model predictions compared with the observed values. Values closer to 0 are indicative of better model performances; the relevant unit is MJ mm/ha/h. (5) Mean absolute error (*MAE*): this is an index that quantifies the discrepancy between the model predictions and the true values. Lower *MAE* values are indicative of higher model accuracies; the relevant unit is MJ mm/ha/h.

The calculations for rainfall erosivity, seasonality analyses, rainfall erosivity model fitting, and precision comparisons were coded in Matlab v.2013b. The geographical map was drawn in ArcGIS v.10.2, and the other figures were drawn in Origin v.9.0.

3 Results and analysis

3.1 Characteristics of erosive rainfall and rainfall erosivity

To avoid invalid contributions of non-erosive rainfall (daily rainfall <12.7 mm) to rainfall erosivity, only erosive rainfall was analyzed in this study. Double-factor variance analysis was applied using SPSS v.17.0 software to statistically assess the influence of stations and months on monthly rainfall erosivity. The results showed that monthly rainfall erosivity values were significantly different (Sig Level < 0.001) at the 99.9% confidence level. However, rainfall erosivity between stations showed no significant difference (Sig Level = 0.552) at this level; hence, the station data could be analyzed together.

Table 3 shows the mean annual erosive rainfall amounts and the mean annual rainfall erosivity at the 5 stations, as well as their CIs. Mean annual erosive rainfall at the 5 stations was 1,076.41 mm, and the standard deviation was 108.45 mm. The range of the CI for the erosive rainfall at the 5 stations was 15.74–17.75, which classifies the erosive rainfall as being between moderately seasonal and highly seasonal. Mean annual rainfall erosivity at the 5 stations was 6,837.37 MJ mm/ha/h/a, and the standard deviation was 615.34 MJ mm ha/h/a. The range of the CI for the rainfall erosivity was 18.99–23.24, which was much higher than that of the erosive rainfall. Clearly, the results indicate that there is a highly concentrated distribution of rainfall erosivity within a year, and high risks for erosion are associated with a centralized period.

Figure 2 illustrates the seasonal distribution of erosive rainfall and rainfall erosivity in Huangshan City. The seasonal distributions were very similar—maximum values both occurred in summer, predominantly June. Erosive rainfall in June was approximately 300 mm

Table 2 Indices and definitions for model performance

Index	Definitions
<i>MAPE</i>	$MAPE = 100 \cdot \bar{P} - \bar{O} / \bar{O}$
<i>ModEff</i>	$ModEff = 1 - \frac{\sum_{i=1}^N (O_i - P_i)^2}{\sum_{i=1}^N (O_i - \bar{O})^2}$
<i>MBE</i>	$MBE = N^{-1} \sum_{i=1}^N (P_i - O_i)$
<i>MAE</i>	$MAE = N^{-1} \sum_{i=1}^N P_i - O_i $

N = number of observations; *O* = observed rainfall erosivity; \bar{O} = mean of observed rainfall erosivity; *P* = predicted rainfall erosivity; \bar{P} = mean of predicted rainfall erosivity.

or 27.18% of the annual erosive rainfall, and this value was higher than the 10.99% value for July. The peak of the seasonal rainfall erosivity also occurred in June, and it reached 2,331 MJ-mm/ha/h, which was 13.52% higher than that of July.

Table 3 Annual erosive rainfall (ER) and annual rainfall erosivity (R) at the 5 stations, as well as their concentration indices (CIs)

Indices	Rucun	Siqian	Taiping	Hezhuang	Wucheng	Mean	SD
Annual ER	1,223.98	925.07	1,038.14	1,094.68	1,100.19	1,076.41	108.45
Annual R	7,749.34	6,900.79	6,089.75	6,506.71	6,940.28	6,837.37	615.34
CI of ER	17.75	16.66	15.74	16.95	17.29	16.88	0.76
CI of R	23.24	18.99	20.51	22.98	19.80	21.10	1.91

SD = standard deviation.
Units: annual ER (mm); annual R (MJ mm ha/h/a); CI is dimensionless

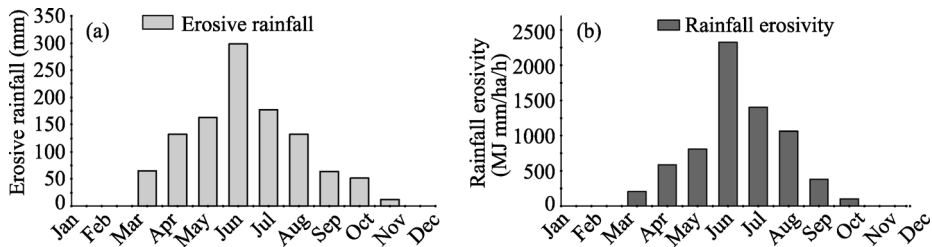


Figure 2 Seasonal distribution of erosive rainfall (a) and rainfall erosivity (b) in Huangshan City

The seasonal distributions of erosive rainfall and rainfall erosivity were closely related to the variations in rainfall events in a year. The mean rainfall amount, mean rainfall intensity, and mean EI_{30} of erosive rainfall events all exhibited pronounced seasonal variations, but with peaks in different months (Figure 3). The maximum amount of mean rainfall occurred in June, while the peak rainfall intensity shifted to July and August, which was the result of the development and intensity of East Asian monsoon rains (Chen, 1983; Tao, 1987; He *et al.*, 2008). Ultimately, the rainfall event represented by EI_{30} , which reflects the combination of the rainfall amount and intensity, had its peak value in June.

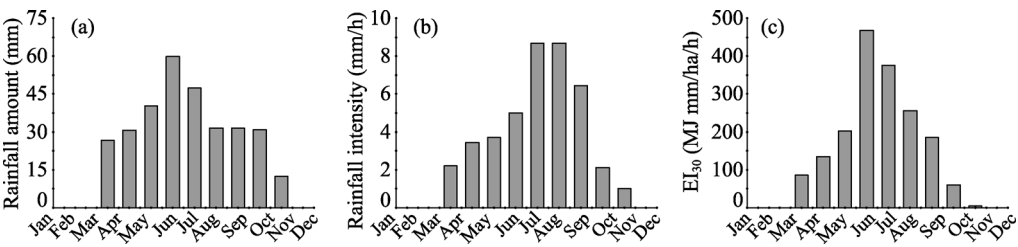


Figure 3 Seasonal distribution of erosive rainfall event characteristics: (a) mean rainfall amount; (b) mean rainfall intensity; (c) mean EI_{30}

3.2 Model parameters

In order to estimate the optimum parameters for each model, the least-squares method was applied to estimate optimal parameters of Model A and the Trust-Region-Reflective algo-

rithm (Coleman and Li, 1996; MathWorks, 2005) was employed in Matlab v.2013b for the derivational models (Model B, Model C, and Model D).

3.2.1 Model A

Table 4 shows the optimal parameters and coefficient of determination r^2 for the Richardson model at the 5 stations in Huangshan City. Figure 4 illustrates the optimal regression results for the Richardson model that were derived from the daily rainfall and daily EI_{30} at the 5 stations in Huangshan City. Daily rainfall and daily EI_{30} were significantly correlated at the 95% confidence level, and r^2 ranged from 0.55 to 0.74 at the 5 stations. The range of parameter α was 1.03–3.09. In comparison with the range of parameter α , parameter β was more stable; its range was between 1.19 and 1.36 at the 5 stations.

Table 4 The optimal parameters from the Richardson model at the 5 stations in Huangshan City

Station	α	β	r^2
Rucun	2.64	1.23	0.71
Siqian	1.03	1.48	0.55
Taiping	1.42	1.36	0.68
Hezhuang	2.29	1.25	0.74
Wucheng	3.09	1.19	0.72

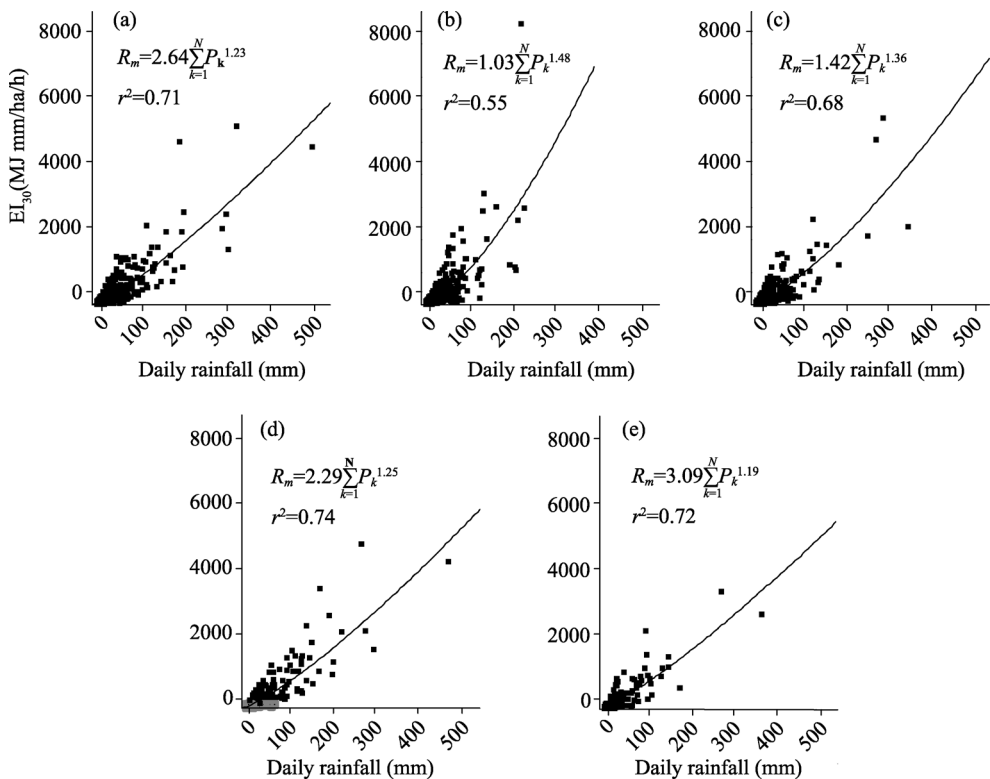


Figure 4 The optimal regression results of the Richardson model from daily rainfall and daily EI_{30} at the 5 stations in Huangshan City: (a) Rucun, (b) Siqian, (c) Taiping, (d) Hezhuang, and (e) Wucheng

3.2.2 Model B

Table 5 displays the optimal parameters of Model B at the 5 stations in Huangshan City. The ranges of parameters α and β were 1.04–3.12 and 1.16–1.46, respectively. The values of the 2 parameters were very close to the values from Model A (the Richardson model), but there

were some differences that may have been influenced by the emergence of the periodic function involved with F_a . Meanwhile, owing to the sensitivity of the exponent in Model B (parameter β), parameter β was lower than that in Model A (the Richardson model) after error minimization.

Table 5 The optimal parameters of Model B at the 5 stations in Huangshan City

Station	α	η_a	β
Rucun	2.23	0.74	1.16
Siqian	1.04	0.13	1.46
Taiping	1.40	0.34	1.32
Hezhuang	2.26	0.26	1.22
Wucheng	3.12	0.16	1.16

Figure 5 presents the seasonal distribution of αF_a at the 5 stations. Pronounced seasonal variations were shown at all of the 5 stations. Although the fluctuation ranges were not the same for the 5 stations, the maximum values all occurred in June, followed by July, and the lowest values were in January and December. Similarly, distribution of αF_a was overall in accordance with the variations in rainfall erosivity in a year, i.e., with maximum rainfall erosivity in June, followed by July, and lower values in winter.

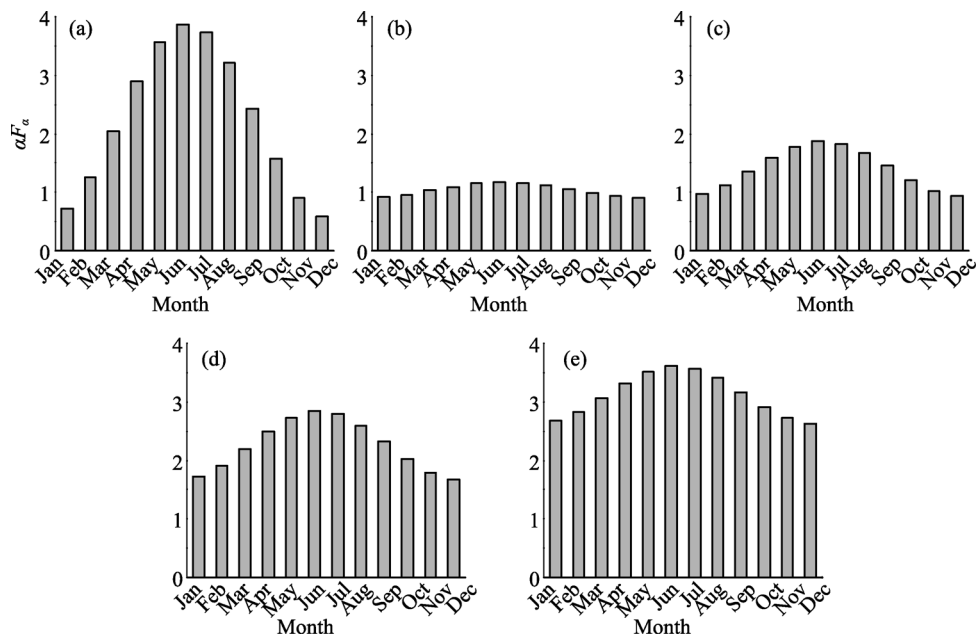


Figure 5 Seasonal distribution of αF_a in Model B at the 5 stations in Huangshan City: (a) Rucun, (b) Siqian, (c) Taiping, (d) Hezhuang, and (e) Wucheng

3.2.3 Model C

The optimal parameters of Model C at the 5 stations in Huangshan City are shown in Table 6. Parameter α ranged from 1.59 to 3.77, and the values were much higher than those from the Richardson model at every station. In contrast, the exponent β values were lower than those of the Richardson model at every station. Its range was 1.05–1.29. Clearly, exponent β needed to be much higher to represent the seasonal variation when parameter α was held constant.

The seasonal distribution of βF_β in Model C at the 5 stations in Huangshan City is illustrated in Figure 6. Variations in βF_β were similar to those of αF_α at every station, whereby June was associated with the peak of βF_β , followed by July, and the minimum value occurred in the winter months. Although the variations were similar, the fluctuation ranges of βF_β in Model C were much smaller than those of αF_α in Model B, and this resulted from the higher sensitivity of the exponent in the power equation.

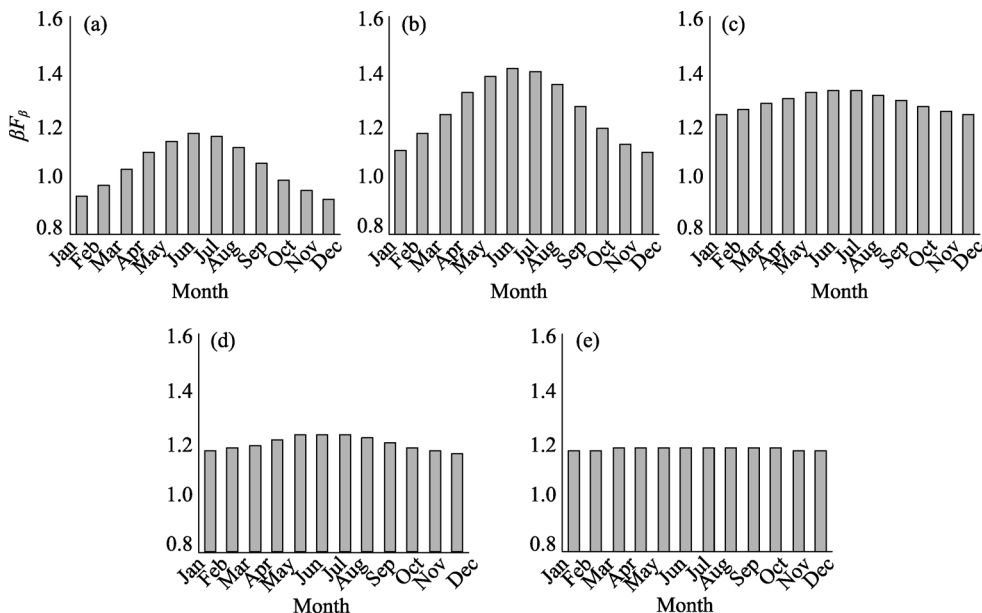


Figure 6 Seasonal distribution of βF_β in Model C at the 5 stations in Huangshan City: (a) Rucun, (b) Siqian, (c) Taiping, (d) Hezhuang, and (e) Wucheng

3.2.4 Model D

Table 7 presents the optimal parameters of Model D at the 5 stations in Huangshan City. Parameter α ranged from 0.82 to 1.79, and these values were much lower than those in the Richardson model at every station. In contrast, exponent β ranged from 1.24 to 1.51, and these values were a bit higher than those in the Richardson model. Although parameter ω_α was set at $5.8\pi/6$, ω_β was not equal to ω_α . On the contrary, error minimization showed that ω_β was much lower than ω_α , which led to a lower ω_β in summer.

Table 6 The optimal parameters of Model C at the 5 stations in Huangshan City

Station	α	β	η_β
Rucun	3.77	1.05	0.11
Siqian	1.59	1.26	0.12
Taiping	1.70	1.29	0.04
Hezhuang	2.61	1.20	0.03
Wucheng	3.16	1.18	0.01

3.3 Comparison of model performance

The performances of the rainfall erosivity models were assessed on an annual and monthly basis. First, we examined the performance on an annual scale by using the annual rainfall erosivity data at the 5 stations. Then, we examined the performance on a monthly scale by using the monthly rainfall erosivity data at the 5 stations and, finally, we examined the

changes for each month at the individual stations (Wucheng).

Figure 7 illustrates the seasonal distributions of $\alpha F\alpha$ and $\beta F\beta$ in Model D. Notably, the seasonal distributions of $\alpha F\alpha$ and $\beta F\beta$ were inverted, which was mainly the result of the co-ordination between the seasonal variations in the 2 parameters.

Table 7 The optimal parameters of Model D at the 5 stations in Huangshan City

Station	α	η_α	β	η_β	ω_β
Rucun	1.79	1.00	1.24	0.06	$1.12\pi/6$
Siqian	0.82	0.51	1.51	0.04	$-0.10\pi/6$
Taiping	0.98	1.00	1.38	0.08	$1.20\pi/6$
Hezhuang	1.30	1.00	1.31	0.08	$1.10\pi/6$
Wucheng	1.57	1.00	1.34	0.12	$-0.36\pi/6$

3.3.1 Annual scale

The *MAPE* and the *ModEff* of the 4 rainfall erosivity models on an annual scale at the 5 stations in Huangshan City are given in Table 8. The performances of the 4 models were all reasonably good, and the performance of Model D was better than that of the other models. For example, the average *MAPE* of Model D was only 3.11%, which was lower than that of the other models, and the smallest *MAPE* values were also found with Model D at 4 out of 5 stations (all except Siqian). Even though the *MAPE* value of Model D at Siqian was not the smallest, the *MAPE* was less than 0.50%. The *ModEff* values showed similar results. The median *ModEff* of Model A and Model D ranked best out of the 4 models, but *ModEff* of Model D showed better performance at more stations than the other models.

Figure 8 illustrates the observed and the model predicted mean annual rainfall erosivity (Figure 8a) along with the *MBE* (Figure 8b) and the *MAE* (Figure 8c) of annual rainfall erosivity at the 5 stations in Huangshan City. The better performance of Model D was further verified. The observed average annual rainfall erosivity of the 5 stations was 6,492.06 MJ mm/ha/h. As can be seen, the prediction by Model D (6,700.15 MJ mm/ha/h) was closer to the observed value of rainfall erosivity than the predictions from the other models. Meanwhile, the closeness between the observed mean annual rainfall erosivity and model predicted results was more obvious at each of the 5 stations. Bar charts of the *MBE* and *MAE* of annual rainfall erosivity also showed the superiority of Model D at more stations compared with the other 3 models.

3.3.2 Monthly scale

Table 9 summarizes the *MAPE* and *ModEff* of the 4 models on a monthly scale at the 5 stations in Huangshan City. Because the *MAPE* of monthly rainfall erosivity was calculated based on the mean value of monthly rainfall erosivity, and the mean value of monthly rainfall erosivity was the mean annual rainfall erosivity divided into data series periods, the *MAPE* of the mean annual rainfall erosivity was equal to the *MAPE* of the mean monthly rainfall erosivity at each station for each model. However, the *ModEff* of monthly rainfall erosivity was not equal to the annual values because it was calculated based on the data for each month in every year, not on the mean value. Although the *ModEff* values of the 4 models seemed good and were nearly equivalent, the *ModEff* values of Model B and Model D

were closer to 1.0, as can be seen from the average value, and the best performance was achieved by Model D at 4 out of the 5 stations (except for Wucheng), thus indicating the better performance of Model D on a monthly scale.

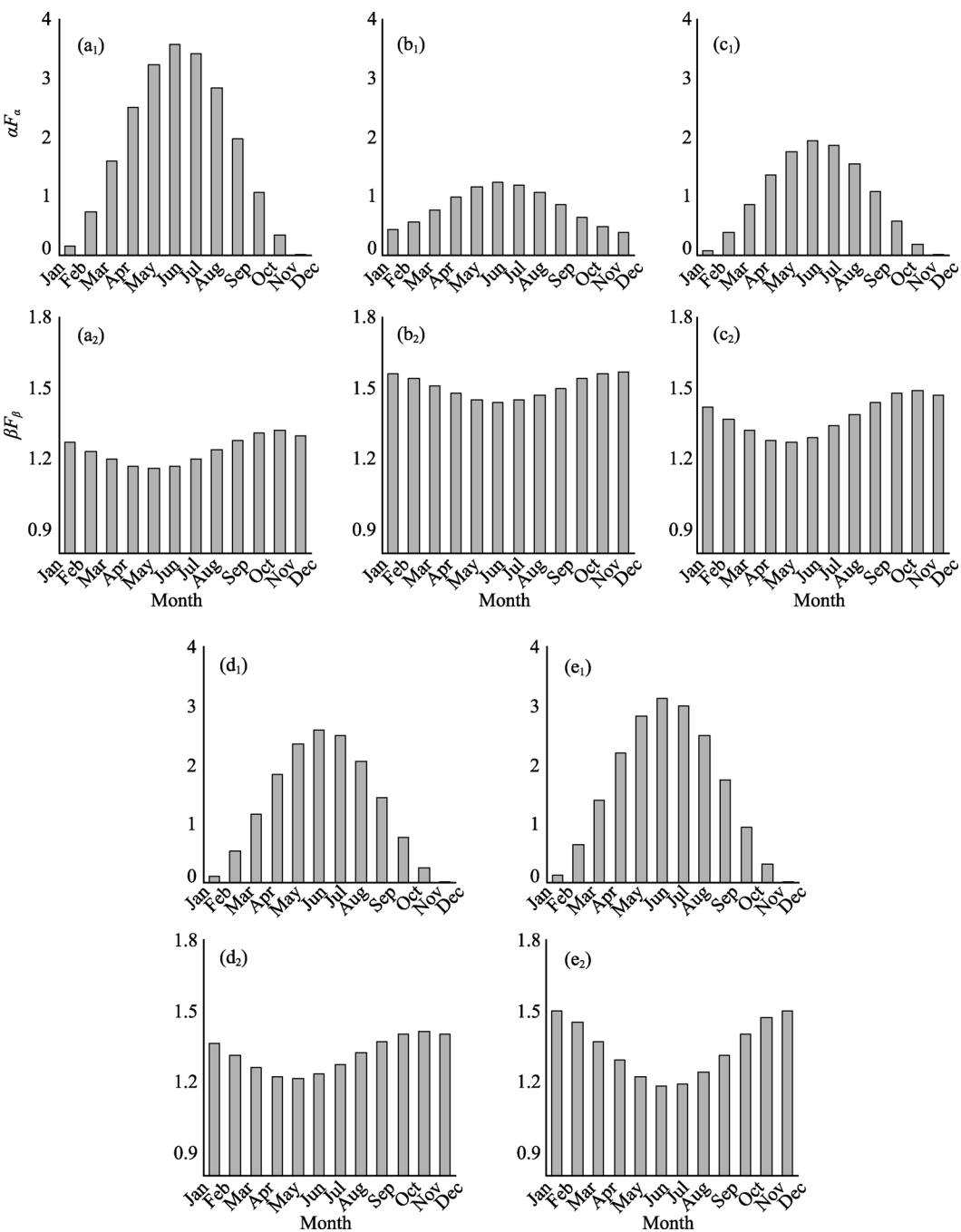


Figure 7 Seasonal distribution of aF_a in Model D at the 5 stations in Huangshan City: (a₁) Rucun, (b₁) Siqian, (c₁) Taiping, (d₁) Hezhuang, and (e₁) Wucheng, and seasonal distribution of βF_β in Model D at the 5 stations in Huangshan City: (a₂) Rucun, (b₂) Siqian, (c₂) Taiping, (d₂) Hezhuang, and (e₂) Wucheng

Table 8 The mean absolute percentage error (*MAPE*) and the model efficiency (*ModEff*) of 4 rainfall erosivity models on an annual scale at the 5 stations in Huangshan City

Parameter	Station	Model A	Model B	Model C	Model D
<i>MAPE</i> (%)	Rucun	6.52	5.15	6.23	5.13
	Siqian	0.18	0.42	1.61	0.38
	Taiping	0.82	1.28	1.64	0.03
	Hezhuang	8.91	9.29	9.54	5.72
	Wucheng	5.80	5.78	5.84	4.29
	Average	4.45	4.38	4.97	3.11
<i>ModEff</i>	Rucun	0.85	0.86	0.85	0.85
	Siqian	0.73	0.73	0.71	0.73
	Taiping	0.80	0.79	0.79	0.82
	Hezhuang	0.86	0.84	0.84	0.86
	Wucheng	0.84	0.84	0.84	0.85
	Average	0.82	0.81	0.81	0.82

The boldface represents the top performance of the 4 models.

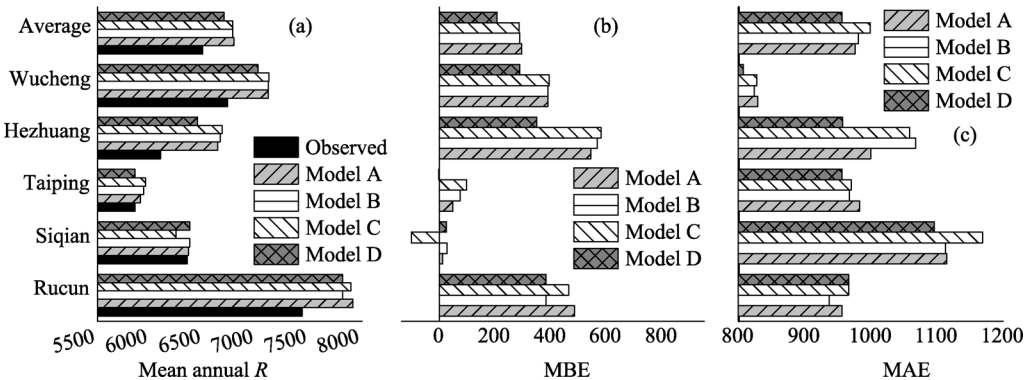


Figure 8 The observed and the model predicted mean annual rainfall erosivity (mean R) (a), the mean bias error (MBE) (b), and the mean absolute error (MAE) (c) of annual rainfall erosivity at the 5 stations in Huangshan City (MJ mm/ha/h/a)

Figure 9 illustrates the observed mean monthly rainfall erosivity (mean R_m) and model predicted results (Figure 9a) along with the MBE (Figure 9b) and the MAE (Figure 9c) of monthly rainfall erosivity at the 5 stations in Huangshan City. At the monthly scale, Model D performed best in terms of the closeness between the observed rainfall erosivity and the predicted values, as well as the lower values of MBE and MAE . This result was similar to that shown at the annual scale for the 4 models.

The performances of the rainfall erosivity models for each month are of importance to the cover-management factor in the USLE and RUSLE calculations. Performances of the models at each station were similar. Thus, we further took Rucun station as a representative site to assess the performances of the models.

The $MAPE$ values for each month from the 4 rainfall erosivity models at Rucun are given in Table 10. Larger errors were found in the months with less rainfall (all months except June and July) compared with the months with more rainfall (June and July). For example, the $MAPE$ values for June and July were both less than 10% for all 4 models (Model A,

Model B, Model C, and Model D). However, the minimum *MAPE* values for the months except for June and July varied among the models. Specifically, the *MAPE* value for Model A was as high as 18.27%, and models B, C, and D yielded values of 12.18%, 5.93%, and 1.62%, respectively, thus suggesting that there was an improvement in the prediction accuracy after seasonal variations in the parameters were incorporated into the models, especially for Model D.

Table 9 The mean absolute percentage error (*MAPE*) and the model efficiency (*ModEff*) of 4 models on a monthly scale at the 5 stations in Huangshan City

Parameter	Station	Model A	Model B	Model C	Model D
<i>MAPE</i> (%)	Rucun	6.52	5.15	6.23	5.13
	Siqian	0.18	0.42	1.61	0.38
	Taiping	0.82	1.27	1.64	0.03
	Hezhuang	8.91	9.29	9.54	5.72
	Wucheng	5.80	5.78	5.84	4.29
	Average	4.45	4.38	4.97	3.11
<i>ModEff</i>	Rucun	0.84	0.85	0.85	0.86
	Siqian	0.74	0.74	0.72	0.74
	Taiping	0.74	0.75	0.75	0.77
	Hezhuang	0.89	0.89	0.89	0.91
	Wucheng	0.85	0.85	0.85	0.84
	Average	0.81	0.82	0.81	0.82

The boldface represents the top performance of the 4 models.

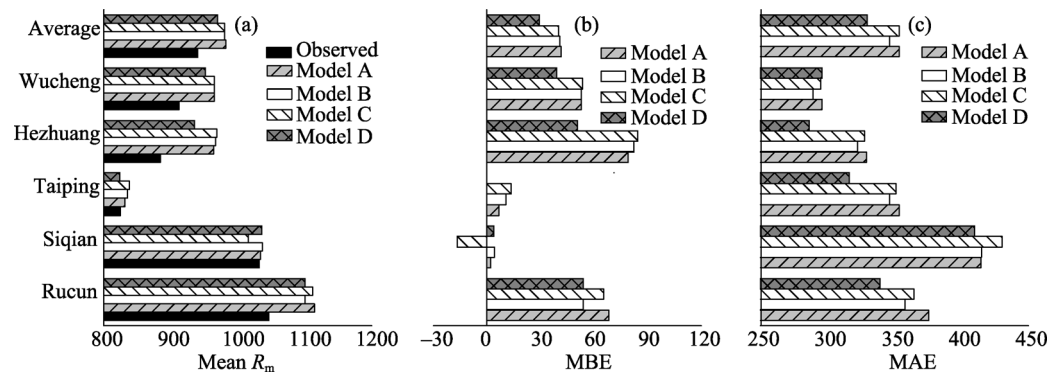


Figure 9 The observed and model predicted mean monthly rainfall erosivity (a), the mean bias error (MBE) (b), and the mean absolute error (MAE) (c) of monthly rainfall erosivity at the 5 stations in Huangshan City (MJ mm/ha/h/a)

The average *MAPE* and the median *MAPE* both verified the improvement of model prediction accuracy after the incorporation of seasonal variations in parameters. The average *MAPE* was 176.76% for the Richardson model (Model A), and it was 48.48% after adding the periodic function F_α to parameter α (Model B), 116.38% after adding the periodic function F_β to parameter β (Model C), and 26.88% after adding the periodic functions F_α and F_β to parameter α and parameter β (Model D), respectively. Clearly, the performance of Model D was best. In order to reduce the influence from the rare occurrences of erosive rainfall in

November during the 20-year analysis period, further evaluation was carried out on the medians of *MAPE* for each month. The median of *MAPE* was 30.42% for Model A, 27.97% for Model B, 31.25% for Model C, and 14.23% for Model D. Slight improvement could be seen with Model B. However, the results were relatively worse for Model C because of its sensitivity. Nevertheless, the best improvement could be found in Model D, and the median of *MAPE* for Model D was about half that of Model A and Model B. Meanwhile, the standard deviations were 372.22%, 81.60%, 258.61%, and 35.44% for Model A, Model B, Model C, and Model D, respectively. These data also demonstrated the improvements of prediction accuracy after incorporating the seasonal variations in parameters, especially for Model D.

Table 10 The mean absolute percentage error (*MAPE*) and significance level (Sig Level) between estimations and EI_{30} values for each month at Rucun

Month	Years	Model A (%, Sig Level)	Model B (%, Sig Level)	Model C (%, Sig Level)	Model D (%, Sig Level)
Mar	11	80.25 (0.005**)	12.18 (0.635)	34.59 (0.199)	1.62 (0.951)
Apr	20	48.52 (0.004**)	27.97 (0.069)	31.25 (0.045*)	14.23 (0.343)
May	20	30.42 (0.001**)	34.08 (0.001**)	32.37 (0.001**)	21.42 (0.013*)
Jun	20	3.79 (0.678)	2.96 (0.745)	2.89 (0.751)	0.51 (0.955)
Jul	19	8.06 (0.416)	2.23 (0.823)	3.16 (0.753)	7.57 (0.412)
Aug	19	25.58 (0.017*)	28.52 (0.011*)	27.70 (0.013*)	15.27 (0.111)
Sep	14	18.27 (0.313)	14.59 (0.368)	5.93 (0.704)	7.37 (0.676)
Oct	18	223.11 (0.001**)	51.87 (0.055)	108.91 (0.002**)	72.65 (0.022*)
Nov	1	1,152.84	261.91	800.66	101.32
Average	16	176.76	48.48	116.38	26.88
Median	19	30.42	27.97	31.25	14.23
SD	6	372.22	81.60	258.61	35.44

The boldface represents the top one performance of the 4 models; * indicates estimations significantly different from EI_{30} at the 0.05 level; ** indicates estimations significantly different from EI_{30} at the 0.01 level.

The *MAPE* of each month further indicated the effectiveness of Model D (Table 10). Specifically, the *MAPE* values of Model A were 80.25% and 48.52% for March and April, respectively. However, they decreased respectively to 12.18% and 27.97% after adding the periodic function F_{α} to parameter α (Model B) or F_{β} to parameter β (Model C), and the decrease was more obvious after further incorporating and coordinating the periodic function F_{α} on parameter α and F_{β} on parameter β in Model D. A similar case could also be found in September, October, and November. However, in May and August, the *MAPE* of Model B increased instead of decreasing, as did that of Model C. In contrast, the predictions of Model D improved—the *MAPE* values of Model D were 1.62%, 14.23%, and 21.42% for March, April, and May, respectively (Table 10), which demonstrated reductions of 78.63%, 34.29%, and 9.00% compared with Model A; the results were also much improved compared with Model B and Model C. In June, July, and August, improvements were also found with respect to Model D compared with the other 3 models.

The model efficiency (*ModEff*) of the 4 rainfall erosivity models for each month at Rucun are shown in Table 11. Model D had a higher efficiency for rainfall erosivity predictions compared to the other models. For example, the median *ModEff* of Model D for all months

was as high as 0.63, and this value was much higher than that of Model B (0.56), Model C (0.54), and Model A (0.46). However, the average *ModEff* of Model B for all months (0.40) was slightly higher than that of Model D, which may have been on account of the low *ModEff* in October that was several magnitudes lower compared with other months (i.e., the average values were affected more by the outlier than the median values). Importantly, the *ModEff* of Model D ranked the highest during 5 (April, May, June, July, and August) out of 8 months, and even during the other months, the *ModEff* of Model D appeared to be better except for October, where the monthly performance was poor because of the high variability of rainfall (it was the highest in the 20-year analysis period).

Figure 10 illustrates the observed and the model predicted mean monthly rainfall erosivity

Table 11 The model efficiency (*ModEff*) of 4 rainfall erosivity models for each month at Rucun

Month	Years	Model A	Model B	Model C	Model D
Mar	11	0.29	0.61	0.54	0.59
Apr	20	0.27	0.47	0.44	0.52
May	20	0.67	0.64	0.66	0.74
Jun	20	0.79	0.79	0.79	0.80
Jul	19	0.82	0.82	0.82	0.84
Aug	19	0.56	0.51	0.51	0.67
Sep	14	0.35	0.48	0.53	0.40
Oct	18	−13.06	−1.16	−3.26	−2.11
Nov	1	–	–	–	–
Average	16	−1.16	0.40	0.13	0.31
Median	19	0.46	0.56	0.54	0.63
Standard deviation	6	4.81	0.64	1.38	0.99

The boldface represents the top performance of the 4 models.

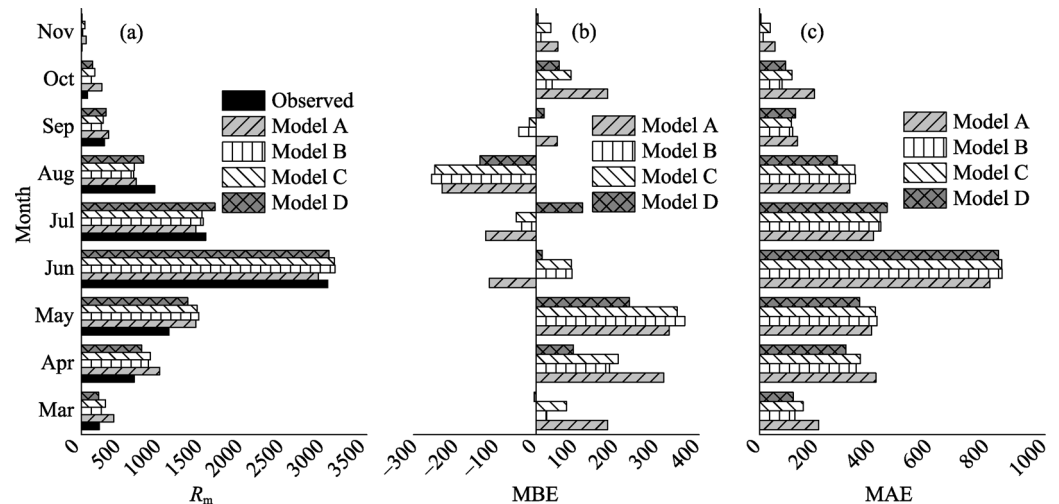


Figure 10 The observed and the model predicted monthly rainfall erosivity (R_m) (a), the mean bias error (MBE) (b), and the mean absolute error (MAE) (c) of monthly rainfall erosivity of the 4 rainfall erosivity models for each month at Rucun (MJ mm/ha/h/a)

(R_m) (Figure 10a) along with the MBE (Figure 10b) and the MAE (Figure 10c) of monthly rainfall erosivity of the 4 models for each month at Rucun station. Better performance of Model D was further supported by the 3 assessment indices overall, especially in the months with less rainfall (March, April, May, August, September, October, and November).

4 Discussion

Sensitivities of parameters in the Richardson model were not the same, which resulted in an unequal response to the same amount of rainfall. Compared with the linear relationship of rainfall erosivity and parameter α , the relationship between rainfall erosivity and the exponent (parameter β) was non-linear, and thus data were more sensitive to rainfall amounts in excess of 12.7 mm, i.e., parameter values much larger than 1.0 (Hamby, 1994). The regression equation at Rucun station was taken as an example to illustrate this tendency (Figure 11). Increasing the value by 0.1 or decreasing it by 0.1 for parameter α only resulted in less than a 5.0% change for the daily rainfall erosivity; however, the change reached nearly 40% for parameter β , which was nearly 8.0 times larger than that of parameter α .

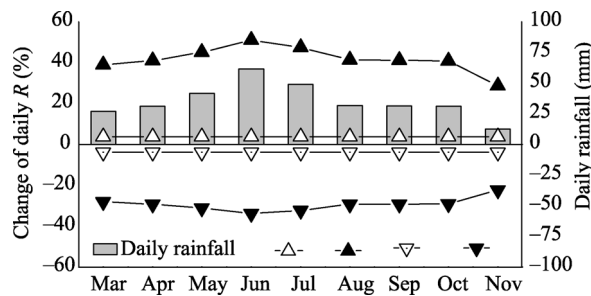


Figure 11 Change of daily R in response to the variations in parameters ($\alpha+0.1$, $\beta+0.1$, $\alpha-0.1$, $\beta-0.1$) for the different months at Rucun station

Furthermore, the change was not the same within the span of a year, and much higher values were observed in the months with more rainfall. This was related to the rainfall characteristics during the year. In summer months, convectional rain was the main form, and this was associated with higher rainfall amounts and heavier intensities that led to more change in the rainfall erosivity. However, in spring or autumn months, frontal rain dominated, and this was associated with lower rainfall amounts and weaker intensities that led to less change in the rainfall erosivity. Consequently, the unequal and cyclical sensitivity of the 2 parameters suggests that it may be possible to disintegrate the parameters from a constant value for the whole year into monthly parameters so as to reduce the model prediction errors, and the results of this study showed that this is feasible.

The addition of a periodic function with a period of 12 months exactly solved the dilemma, i.e., it could effectively differentiate the unequal contribution of rainfall in a year. There were clear seasonal variations in αF_{α} , and the maximum value occurred in June, followed by July. Similar variations in αF_{α} have been verified in Finland (Posch and Rekolainen, 1993), northeast Spain (Posch and Rekolainen, 1993), Australia (Lu and Yu, 2002), and New South Wales in Australia (Yu and Rosewell, 1996; Yang, 2014), as well as in China (Zhu and Yu, 2015). For parameter β , both Angulo-Martinez and Begueria (2009) and

Ramos and Duran (2014) have verified its seasonal variations in northeast Spain, and the results were similar to those of this study; even seasonal variations in βF_β have been considered (Richardson *et al.*, 1983; Bagarello and Dasaro, 1994; Petkovsek and Mikos, 2004). When the 2 parameters are both incorporated into the model, theoretically, the results should be much better than the models that incorporate the seasonal variations in only 1 parameter (parameter α or β). In the latter models, either αF_α or βF_β is considered to be constant throughout the year, while the other varies seasonally. The key is the coordination between seasonal variations in the 2 parameters (αF_α and βF_β). Due to the unequal sensitivity of the 2 parameters (parameter α and β) and the higher sensitivity of parameter β in June, lower values should prevail in the months with more rainfall, i.e., June and July. Meanwhile, αF_α and βF_β are closely related to each other (Zhu and Yu, 2015). Naturally, higher values of αF_α also occur in the months with more rainfall, and the coordination of αF_α and βF_β can thus be set up, which has the potential to minimize the prediction errors for rainfall erosivity.

Each month's prediction accuracies for the model that only incorporated seasonal variations in parameter α (Model B) were much better than those for the model that did not consider any seasonal variations in the parameters (Model A) as a whole. Compared with Model B, the performance of Model C was worse, and this was the result of the high sensitivity of exponent parameter β . However, the performance of Model D for each month, which incorporated and coordinated the seasonal variations in both parameters α and β , was overall much better than that of Model A, Model B, and Model C. Besides, the model prediction accuracy on an annual scale was well maintained or even improved. The improvement in the model prediction accuracy can be explained by the following 2 factors. (1) The model considered the seasonal variations in both parameters α and β . The seasonal characteristics of rainfall and rainfall erosivity permit the possibility of mathematical modeling, and variations in the 2 parameters were well represented by the addition of the periodic function. (2) There was coordination between the seasonal variations in parameters α and β . The discordant sensitivity of parameters α and β enabled the model predicted errors to be minimized by coordinating the variations in parameters. The maximum parameter αF_α occurred in June, which coincided with the maximum rainfall during the year. At the same time, the inverse variation of βF_β enabled errors to be minimized during the month with higher rainfall, and this approach represents a new way to solve the discordant sensitivity of parameters issue in geographic modeling.

In contrast to the Yu and Rosewell model (Model A), 2 more variables that incorporated and coordinated the seasonal variations in both parameters α and β were introduced in Model D, and an improvement in the rainfall erosivity estimation for each month was achieved. Meanwhile, higher prediction accuracy was maintained on an annual scale. In terms of the application of the models on a monthly scale, priority should be given to the model that incorporates and coordinates seasonal variations in both parameters α and β (Model D), but the Richardson model (Model A) can still be recommended when only an estimation of the rainfall erosivity on an annual scale is required.

5 Conclusions

On the basis of high-resolution pluviographic data at 5 stations in Huangshan City, this pa-

per tested and validated models that incorporated seasonal variations in parameters α and β into the basic Richardson model. The results were as follows.

(1) Medium to high seasonality of erosive rainfall and rainfall erosivity were found at 5 stations (Rucun, Siqian, Taiping, Hezhuang and Wucheng) in Huangshan City, and higher seasonality was found in the rainfall erosivity. Seasonal distributions of erosive rainfall and rainfall erosivity were similar—maximum erosive rainfall and rainfall erosivity occurred in June, which is when erosive rainfall accounted for nearly 27.18% of the annual erosive rainfall, and the percentage reached 33.85% for the rainfall erosivity.

(2) Seasonal variations in parameters α and β of the Richardson model were well represented.

(3) The model that incorporated and coordinated the seasonal variations in both parameters α and β into the Richardson model was more effective than the other models when estimating rainfall erosivity for each month, and higher prediction accuracies were maintained on an annual scale with this model.

(4) Priority should be given to the model that incorporates and coordinates seasonal variations in both parameters α and β when monthly rainfall-erosivity data are needed, but the Richardson model can still be recommended when only an estimation of the rainfall erosivity on an annual scale is required.

This study has provided new insight into the process of seasonal rainfall erosivity modeling, and a rainfall erosivity model that incorporates and coordinates seasonal variations in 2 parameters on the basis of the Richardson model was tested and proven to be more effective than other models for predicting monthly rainfall erosivity. Such data will be important for improving cover-management factor calculations and soil loss estimations for soil erosion risk assessments under different climate-change scenarios, but further validation of the model is needed at additional stations.

Acknowledgments

We want to express our gratitude to the respected anonymous reviewers that led to improve the original manuscript. Their valuable and constructive suggestions are greatly appreciated.

References

- Angulo-Martinez M, Begueria S, 2009. Estimating rainfall erosivity from daily precipitation records: A comparison among methods using data from the Ebro Basin (NE Spain). *Journal of Hydrology*, 379(1/2): 111–121.
- Bagarello V, Dasaro F, 1994. Estimating single storm erosion index. *Transactions of the ASAE*, 37(3): 785–791.
- Bonilla C A, Vidal K L, 2011. Rainfall erosivity in Central Chile. *Journal of Hydrology*, 410(1/2): 126–133.
- Chen G T-J, 1983. Observational aspects of the Mei-Yu phenomena in subtropical China. *Journal of the Meteorological Society of Japan*, 61: 306–312.
- Coleman T F, Li Y Y, 1996. A reflective Newton method for minimizing a quadratic function subject to bounds on some of the variables. *SIAM Journal on Optimization*, 6(4): 1040–1058.
- Davison P, Hutchins M G, Anthony S G *et al.*, 2005. The relationship between potentially erosive storm energy and daily rainfall quantity in England and Wales. *Science of the Total Environment*, 344(1–3): 15–25.
- Diodato N, Bellocchi G, 2007. Estimating monthly (R)USLE climate input in a Mediterranean region using limited data. *Journal of Hydrology*, 345(3/4): 224–236.b

- Eltaif N I, Gharaibeh M A, Al-Zaitawi F *et al.*, 2010. Approximation of rainfall erosivity factors in North Jordan. *Pedosphere*, 20(6): 711–717.
- Foster G R, 2004. Revised Universal Soil Loss Equation Version 2: User reference guide. USDA Natural Resources Conservation Service, Tennessee.
- Guo Q K, Liu B Y, Xie Y *et al.*, 2015. Estimation of USLE crop and management factor values for crop rotation systems in China. *Journal of Integrative Agriculture*, 14(9): 1877–1888.
- Guo X B, Wang Z Q, Zhang R L, 2001. Study on temporal distribution of rainfall erosivity and daily rainfall erosivity model in red soil area of Zhejiang. *Journal of Soil and Water Conservation*, 15(3): 35–35. (in Chinese)
- Hamby D M, 1994. A review of techniques for parameter sensitivity analysis of environmental models. *Environmental Monitoring and Assessment*, 32(2): 135–154.
- He J H, Zhao P, Zhu C W *et al.*, 2008. Discussions on the East Asian subtropical monsoon. *Acta Meteorologica Sinica*, 66(5): 683–696.
- Hoyos N, Waylen P R, Jaramillo Á, 2005. Seasonal and spatial patterns of erosivity in a tropical watershed of the Colombian Andes. *Journal of Hydrology*, 314(1–4): 177–191.
- Kavian A, Fathollah N Y, Habibnejad M *et al.*, 2011. Modeling seasonal rainfall erosivity on a regional scale: A case study from northeastern Iran. *International Journal of Environmental Research*, 5(4): 939–950.
- Kinnell P I A, 2010. Event soil loss, runoff and the Universal Soil Loss Equation family of models: A review. *Journal of Hydrology*, 385(1–4): 384–397.
- Lal R, 2003. Soil erosion and the global carbon budget. *Environment International*, 29(4): 437–450.
- Lee J H, Heo J H, 2011. Evaluation of estimation methods for rainfall erosivity based on annual precipitation in Korea. *Journal of Hydrology*, 409(1/2): 30–48.
- Lu H, Yu B F, 2002. Spatial and seasonal distribution of rainfall erosivity in Australia. *Australian Journal of Soil Research*, 40(6): 887–901.
- Mannaerts C M, Gabriels D, 2000. Rainfall erosivity in Cape Verde. *Soil & Tillage Research*, 55(3/4): 207–212.
- MathWorks I, 2005. MATLAB: The language of technical computing. Desktop Tools and Development Environment, version 7, MathWorks
- Mati B M, Morgan R P, Gichuki F N *et al.*, 2000. Assessment of erosion hazard with the USLE and GIS: A case study of the Upper Ewaso Ng'iro North basin of Kenya. *International Journal of Applied Earth Observation and Geoinformation*, 2(2): 78–86.
- McGregor K C, Mutchler C K, 1976. Status of the R factor in Northern Mississippi. *Soil Erosion: Prediction and Control*, *Soil Conservation Soc. Amer.*, 135–142.
- Mikhailova E A, Bryant R B, Schwager S J *et al.*, 1997. Predicting rainfall erosivity in Honduras. *Soil Science Society of America Journal*, 61(1): 273–279.
- Nash J E, Sutcliffe J V, 1970. River flow forecasting through conceptual models (Part I): A discussion of principles. *Journal of Hydrology*, 10(3): 282–290.
- Ning L D, Shi H, 2003. Estimating R-factor in Southwest China with data of daily rainfall amount. *Research of Soil and Water Conservation*, 10(4): 183–186. (in Chinese)
- Oliver J E, 1980. Monthly precipitation distribution: A comparative index. *Professional Geographer*, 32(3): 300–309.
- Petkovsek G, Mikos M, 2004. Estimating the R factor from daily rainfall data in the sub-Mediterranean climate of southwest Slovenia. *Hydrological Sciences Journal-Journal Des Sciences Hydrologiques*, 49(5): 869–877.
- Pimentel D, Harvey C, Resosudarmo P *et al.*, 1995. Environmental and economic costs of soil erosion and conservation benefits. *Science-AAAS-Weekly Paper Edition*, 267(5201): 1117–1122.
- Posch M, Rekolainen S, 1993. Erosivity factor in the Universal Soil Loss Equation estimated from Finnish rainfall data. *Agricultural Science in Finland*, 2(4): 271–279.
- Ramos M C, Duran B, 2014. Assessment of rainfall erosivity and its spatial and temporal variabilities: Case study of the Penedes area (NE Spain). *Catena*, 123: 135–147.
- Renard K G, Foster G R, Weesies G A *et al.*, 1997. Predicting Soil Erosion by Water: A Guide to Conservation

- Planning with the Revised Universal Soil Loss Equation (RUSLE). Washington: USDA.
- Renard K G, Freimund J R, 1994. Using monthly precipitation data to estimate the R-factor in the revised USLE. *Journal of Hydrology*, 157(1): 287–306.
- Richardson C W, Foster G R, Wright D A, 1983. Estimation of erosion index from daily rainfall amount. *Transactions of the ASAE*, 26(1): 153–156.
- Salako F K, 2010. Development of iseroindent maps for Nigeria from daily rainfall amount. *Geoderma*, 156(3/4): 372–378.
- Sanchez-Moreno J F, Mannaerts C M, Jetten V, 2014. Rainfall erosivity mapping for Santiago Island, Cape Verde. *Geoderma*, 217: 74–82.
- Selker J S, Haith D A, Reynolds J E, 1990. Calibration and testing of a daily rainfall erosivity model. *Transactions of the ASAE*, 33(5): 1612–1618.
- Shamshad A, Azhari M N, Isa M H *et al.*, 2008. Development of an appropriate procedure for estimation of RUSLE EI30 index and preparation of erosivity maps for Pulau Penang in Peninsular Malaysia. *Catena*, 72(3): 423–432.
- Taguas E V, Carpintero E, Ayuso J L, 2013. Assessing land degradation risk through the long-term analysis of erosivity: A case study in southern Spain. *Land Degradation & Development*, 24(2): 179–187.
- Tao S Y, 1987. A review of recent research on the East Asian summer monsoon in China. *Monsoon Meteorology*.
- Wischmeier W H, Smith D D, 1958. Rainfall energy and its relationship to soil loss. *Eos, Transactions American Geophysical Union*, 39(2): 285–291.
- Wischmeier W H, Smith D D, 1978. Predicting Rainfall Erosion Losses: A Guide to Conservation Planning. Washington: USDA.
- Yang X H, 2014. Deriving RUSLE cover factor from time-series fractional vegetation cover for hillslope erosion modelling in New South Wales. *Soil Research*, 52(3): 253–261.
- Yu B, 1998. Rainfall erosivity and its estimation for Australia's tropics. *Australian Journal of Soil Research*, 36(1): 143–165.
- Yu B, Hashim G M, Eusof Z, 2001. Estimating the R-factor with limited rainfall data: A case study from Peninsular Malaysia. *Journal of Soil and Water Conservation*, 56(2): 101–105.
- Yu B, Rosewell C J, 1996. An assessment of a daily rainfall erosivity model for New South Wales. *Australian Journal of Soil Research*, 34(1): 139–152.
- Yu B, Rosewell C J, 1996. Rainfall erosivity estimation using daily rainfall amounts for South Australia. *Australian Journal of Soil Research*, 34(5): 721–733.
- Yu B F, Neil D T, 2000. Empirical catchment-wide rainfall erosivity models for two rivers in the humid tropics of Australia. *Australian Geographer*, 31(1): 115–132.
- Zhu Z L, Yu B F, 2015. Validation of rainfall erosivity estimators for mainland of China. *Transactions of the ASABE*, 58(1): 61–71.